Electro-Optical Switch Using $Ge_2Sb_2Te_5$ Phase-Change Material in a Silicon MZI Structure

Hanyu Zhang[1], Linjie Zhou[1]*, Liangjun Lu[1], Zhanzhi Guo[1], Jian Xu[2], Xuecheng Fu[2], Jianping Chen[1] and B. M. A. Rahman[3]

[1]State Key Laboratory of Advanced Optical Communication Systems and Networks, Department of Electronic Engineering
Shanghai Jiao Tong University, Shanghai 200240, P. R. China
[2]Advanced Electronics Materials and Devices
Shanghai Jiao Tong University, Shanghai 200240, P. R. China
[3]Department of Electrical and Electronic Engineering,
City University London, Northampton Square, London EC 1V 0HB, U.K.
*ljzhou@sjtu.edu.cn

Abstract—**We report a novel silicon MZI switch activated by the phase change of a sub-micrometer-size $Ge_2Sb_2Te_5$ (GST) thin film. The phase change of GST is triggered by electrical pulses, leading to two "self-holding" switching states. Extinction ratio change of 5-dB is measured from the MZI spectrum.**

Keywords-phase change material; optical switching device; integrated optics devices

I. INTRODUCTION

To make a large-scale photonic integrated circuit, the individual optical components should be as compact as possible to reduce the chip footprint and power consumption. Silicon-on-insulator based photonic devices are extremely attractive due to its compactness and compatibility with microelectronic circuits using the well-developed CMOS technology. Actively tunable devices are inevitably required to build complex integrated chips in many applications. The active tuning in silicon is usually realized by the thermo-optic [1] or free-carrier plasma dispersion [2] effects. However, the thermal effect is slow in the order of microsecond. The free-carrier effect, on the other hand, is fast but relatively weak with a refractive index change only in the order of 0.001 and moreover loss also increases with free-carriers injection. Resonant structures, such as ring resonators [3], disk resonators [4], Bragg gratings [5] and photonic crystals [6], can be employed to reduce the device size. However, this is achieved with the sacrifice of the optical bandwidth, and moreover, the resonant devices are quite sensitive to temperature change [7], leading to potential stability issue.

One solution to overcome the fundamental limitation in today's silicon photonic devices is to use exotic materials with a much larger refractive index modulation. The phase-change material (PCM) is one of the materials that can serve for this purpose. There exist at least two phases with significantly different optical properties, which can be repeatedly and rapidly cycled. The $Ge_2Sb_2Te_5$ (GST) is a widely-used PCM in which the phase change can be thermally, optically or electrically induced potentially with an ultrahigh speed [8] [9]. The GST possesses the "self-holding" feature [10], and consequently there is no static power consumption to maintain the states. Here, we report on the first experimental demonstration of optical switching in a silicon Mach-Zehnder interferometer (MZI) structure integrated with electrically-driven GST as the active material.

II. EXPERIMENTAL IMPLEMENTATION

A. Device structure

Figure 1(a) shows the schematic structure of an asymmetric MZI with one arm waveguide partially covered with a stack of Indium Tin Oxides (ITO)/GST/ITO film. The MZI is composed of a pair of 1×2 multimode interferometers (MMIs) with a 3-dB coupling ratio. The arm waveguide length difference is 166 μm. Figure 1(b) shows the magnified view of the active waveguide. The ITO and GST/ITO patches are overlapped on top of the waveguide with an area of 0.75×0.75 μm^2. The GST is sandwiched between the two ITO layers as illustrated by the cross-section in Fig. 1(c). The top and bottom ITO layers are used as electrodes so that voltage can be applied onto the GST film in this capacitor structure. The ITO also protects the GST from being oxidized when exposed in the air. The ITO/GST/ITO layer thickness is 60/50/60 nm.

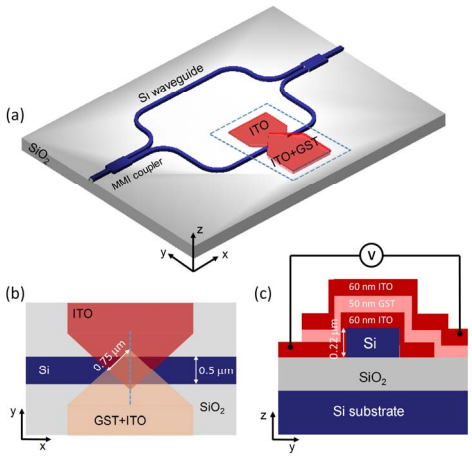

Fig. 1. (a) Schematic structure of the optical switch using GST. (b) Top view of the ITO/GST/ITO covered active silicon waveguide. (c) Cross-section of the active waveguide.

The working principle of the device is described as follows. The GST changes from the amorphous (am) state to the crystalline (cr) state and vice versa upon an external electrical pulse. The complex refractive index of the GST at a wavelength of 1550 nm is 4.6 + 0.12i for the crystalline state and 7.45 + 1.49i for the amorphous state [11]. The GST phase change influences the effective index of the active waveguide, and as a result, the MZI output spectrum changes. Figure 2 illustrates the electric field distribution of the fundamental quasi-transverse electric (TE) modes in the active waveguide when the GST is at amorphous and crystalline states. The ITO is assumed to have a refractive index of 1.8+0.03i [12]. The calculated effective indices of the active waveguide are $n_{eff\,(am)}$ = 2.74+0.028i and $n_{eff\,(cr)}$ = 2.411+0.129i. It reveals that the crystalline state has a smaller propagation constant and a higher optical absorption loss. It should be noted that the GST has a self-holding characteristic, and therefore the two states can be maintained without any electrical supply. Electrical power is only consumed during the dynamic phase change process, leading to much lower power consumption if the switching frequency is low.

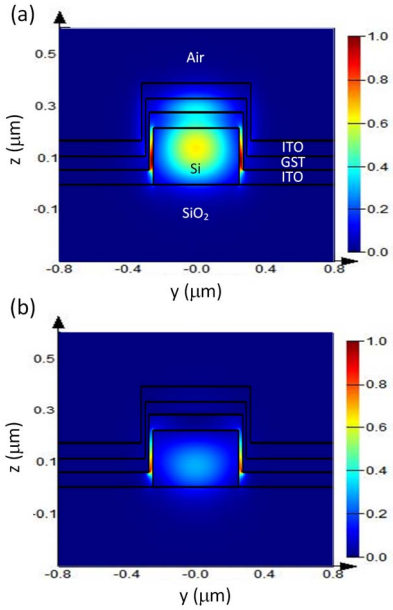

Fig. 2. Simulated electric-field intensity profiles of the active waveguide when the GST is at (a) the amorphous state and (b) the crystalline state.

B. *Device fabrication*

Figure 3(a) shows the device fabrication process flow. It began with a silicon-on-insulator wafer with a top silicon layer thickness of 220 nm and a buried oxide (BOX) layer thickness of 2 μm. The silicon waveguides were patterned by e-beam lithography (EBL) followed by reactive ion etch (RIE). Then a lift-off process was used to deposit the bottom ITO. Next, a second lift-off process was performed to form the top GST/ITO layers. The ITO/GST/ITO layers wrap around the silicon waveguide to interact effectively with the waveguide mode. The GST and ITO layers were deposited using the sputtering method, ensuring the good waveguide sidewall coverage by the thin films. Figure 3(b) shows the optical microscope image of the fabricated device.

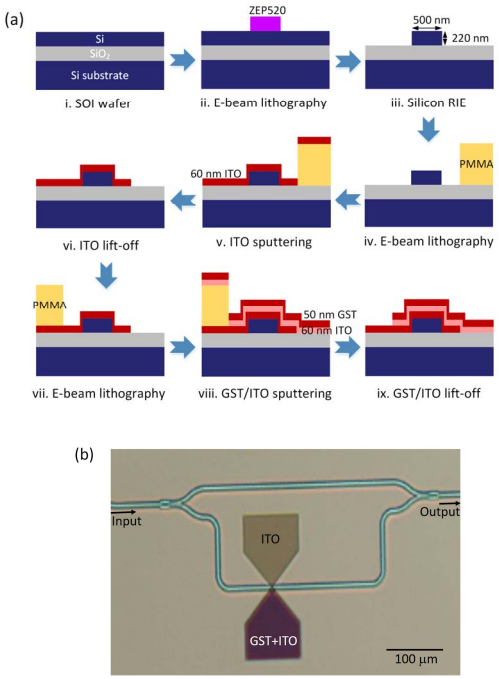

Fig. 3. (a) Device fabrication process flow. (b) Microscope image of the fabricated device.

C. *Experimental results*

We first measured the current-voltage (I-V) curves of the ITO/GST/ITO stack for two successive cycles as shown in Fig. 4. In the measurement, the current was swept while the voltage was recorded. The as-deposited GST material is initially at the amorphous state. Therefore, in the beginning of the first cycle, the GST exhibits a large resistance. When the voltage gradually increases to the GST phase change threshold voltage V_T [13], it suddenly drops back to a lower value, implying the GST resistance reduces considerably. This is a clear indication of the phase change of the GST material. In the second cycle, the measured I-V curve is a linear line with low resistance. The bandgap energy of GST is around 0.7 eV and 0.5 eV in the amorphous and crystalline states, respectively [13]. The amorphous GST hence behaves more like an intrinsic semiconductor, while the crystalline GST has a higher concentration of free-carriers with good electrical conductivity.

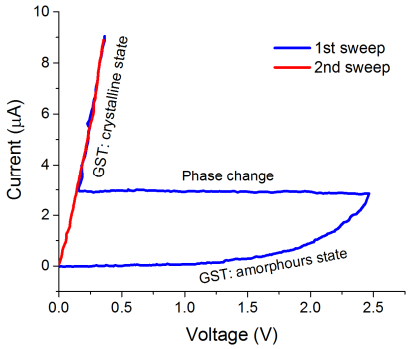

Fig. 4. I-V curve measurement before and after GST phase change.

We next performed the phase change experiment with electrical pulses. The pulses were generated from an arbitrary waveform generator (AWG) and applied to the ITO electrodes via a pair of metal probes. The amorphization of GST was enabled by using a reset pulse with a width of 100 ns and a peak voltage of 8 V. The recrystallization of GST was obtained by a set pulse with a width of 500 ns and a peak voltage of 3 V. The effect of phase change was examined by measuring the TE transmission spectrum of the MZI. Figure 5(a) shows the normalized spectra for two phase change cycles (two crystalline states and two amorphous states). The free-spectral range (FSR) is 3.2 nm. Both of the amorphous and crystalline states can be well recovered after several cycles. Fig. 5(b) illustrates the magnified spectra in one FSR. Two effects can be clearly discerned by comparison of the two spectra. The amorphous state shows a red-shifted spectrum and a higher extinction ratio (ER). This was expected since the amorphous state has a larger real refractive index but a smaller imaginary index, as given by the simulation in Fig. 2.

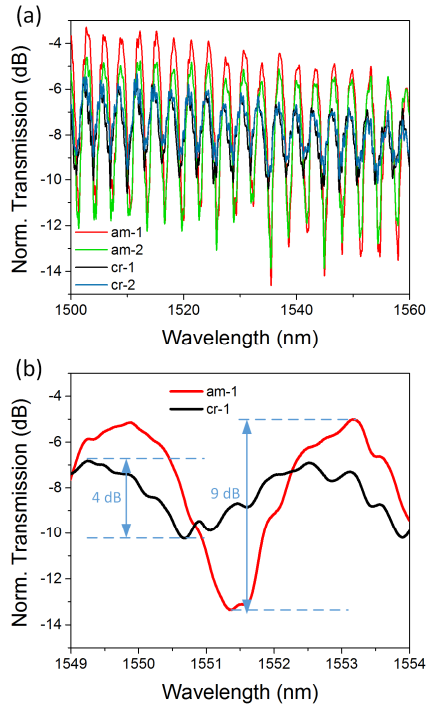

Fig. 5. (a) Measured transmission spectra of the MZI in two cycles of GST phase change. (b) Magnified spectra in one FSR.

III. CONCLUSIONS

We have experimentally demonstrated a MZI optical switch based on the phase change of electrically-driven GST. The ITO/GST/ITO stack layer area on top of the silicon waveguide is less than 1 μm^2. Preliminary experimental results reveal that the GST can undergo repeatable phase change induced by electrical pulses. The phase change has a significant effect on the optical performance of the MZI switch. The extinction ratio varies by 5 dB. The proof-of-principle experiment proves the possibility of hybrid integration of GST with silicon waveguides for potential ultra-compact photonic integration.

ACKNOWLEDGMENT

This work was supported in part by 61661130155, 61422508. We acknowledge the Advanced Electronic Materials and Devices (AEMD) platform at SJTU for device fabrication. We also thank Dr. Richard A. Soref for the insightful discussion.

REFERENCES

[1] S. Zhao, L. Lu, L. Zhou, D. Li, Z. Guo, and J. Chen, "16x16 silicon Mach-Zehnder interferometer switch actuated with waveguide microheaters," *Photon. Res.,* vol. 4, pp. 202-207, 2016/10/01 2016.

[2] L. Lu, S. Zhao, L. Zhou, D. Li, Z. Li, M. Wang, *et al.*, "16x16 non-blocking silicon optical switch based on electro-optic Mach-Zehnder interferometers," *Opt. Express,* vol. 24, pp. 9295-9307, 2016.

[3] W. Bogaerts, P. D. Heyn, T. V. Vaerenbergh, K. D. Vos, S. K. Selvaraja, T. Claes, *et al.*, "Silicon microring resonators," *Laser Photon. Rev.,* vol. 6, pp. 47–73, 2012.

[4] H. Zhu, L. Zhou, R. Yang, X. Li, and J. Chen, "Enhanced Near-Infrared Photodetection with Avalanche Gain in Silicon Microdisk Resonators Integrated with PN Diodes," *Optics Letters,* vol. 39, pp. 4525-4528, 2014.

[5] Z. Zou, L. Zhou, X. Li, and J. Chen, "60-nm-thick basic photonic components and Bragg gratings on the silicon-on-insulator platform," *Opt. Express,* vol. 23, pp. 20784-20795, 2015/08/10 2015.

[6] S. Fan and J. D. Joannopoulos, "Analysis of guided resonances in photonic crystal slabs," *Phys. Rev. B,* vol. 65, pp. 121-121, 2002.

[7] L. Zhou, K. Okamoto, and S. J. B. Yoo, "Athermalizing and trimming of slotted silicon microring resonators with UV-sensitive PMMA upper-cladding," *IEEE Photon.Technol. Lett.,* vol. 21, pp. 1175-1177, 2009.

[8] F. Xiong and E. Pop, "Low-power switching of phase-change materials with carbon nanotube electrodes," *Science,* vol. 332, pp. 568-70, 2011.

[9] S. H. Lee, Y. Jung, and R. Agarwal, "Highly scalable non-volatile and ultra-low-power phase-change nanowire memory," *Nat. Nanotechnol.,* vol. 2, pp. 626-30, 2007.

[10] R. Soref, "Phase-change materials for Group-IV electro-optical switching and modulation," in *2015 IEEE 12th International Conference on Group IV Photonics (GFP)*, 2015, pp. 157-158.

[11] H. Liang, R. Soref, J. Mu, and A. Majumdar, "Simulations of Silicon-on-Insulator Channel-Waveguide Electrooptical 2 × 2 Switches and 1 × 1 Modulators Using a Self-Holding Layer," *J. Lightwave Technol.* , vol. 33, pp. 1805-1813, 2015.

[12] F. Yi, E. Shim, A. Y. Zhu, H. Zhu, J. C. Reed, and E. Cubukcu, "Voltage tuning of plasmonic absorbers by indium tin oxide," *Appl. Phys. Lett.,* vol. 102, pp. 221102-221102-4, 2013.

[13] S. Raoux, F. Xiong, M. Wuttig, and E. Pop, "Phase change materials and phase change memory," *MRS Bulletin,* vol. 39, pp. 703-710, 2014.